

## Interconversion of $\text{ROC}^+$ and $\text{RCO}^+$ ( $\text{R} = \text{H}$ and $\text{CH}_3$ ): Gas-Phase Catalysis by Argon and Dinitrogen

Alwin Cunje, Christopher F. Rodriguez, Diethard K. Bohme, and Alan C. Hopkinson\*

Department of Chemistry, York University, North York, Ontario, Canada M3J 1P3

Received: August 13, 1997; In Final Form: October 31, 1997<sup>⊗</sup>

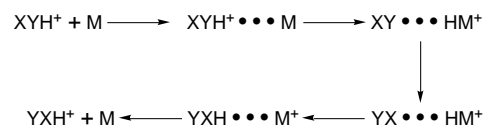
Molecular orbital calculations using density functional theory at the B3LYP/6-311++G(d,p) level have been used to optimize structures for ions  $\text{COR}^+\cdots\text{M}$  and  $\text{M}\cdots\text{RCO}^+$  and also for the transition structures  $\text{COR}^+\cdots\text{M}$ -(ts) for their interconversion ( $\text{R} = \text{H}$ ,  $\text{CH}_3$  and  $\text{M} = \text{Ar}$  and  $\text{N}_2$ ). For the unsolvated ions and for ions  $\text{COH}^+\cdots\text{M}$ ,  $\text{M}\cdots\text{HCO}^+$ , and  $\text{COH}^+\cdots\text{M}$ (ts) the optimized structures were used for single-point calculations at QCISD(T)(full)/6-311++G(2df,p). Critical points on the  $\text{COH}^+$  and  $\text{ArCOH}^+$  potential energy surfaces were also optimized at MP2(full)/6-311++G(3df,3pd). For the uncomplexed ions  $\text{COR}^+$ , the barriers to 1,2-migration of  $\text{R}^+$  at B3LYP/6-311++G(d,p) are 35.4 kcal mol<sup>-1</sup> for  $\text{R} = \text{H}$  and 14.2 kcal mol<sup>-1</sup> for  $\text{R} = \text{CH}_3$ . Inclusion of a dinitrogen molecule removes this barrier by permitting  $\text{COR}^+$  to deposit  $\text{R}^+$  on  $\text{N}_2$  followed by CO retrieving the  $\text{R}^+$  to produce the lower energy isomer,  $\text{RCO}^+$ . Argon has a lower  $\text{R}^+$  affinity than the oxygen atom of CO and does not remove  $\text{R}^+$  from  $\text{COR}^+$ . Preferential stabilization by argon of the transition structure for the 1,2-migration of  $\text{R}^+$  over stabilization of  $\text{COR}^+$  at the minimum results in a reduction in the barrier to rearrangement. The gas-phase rearrangements of ions  $\text{COR}^+$  via “solvated” transition structures  $\text{COR}^+\cdots\text{Ar}$ (ts) are calculated to have barriers of 8.3 kcal mol<sup>-1</sup> for  $\text{R} = \text{H}$  and 5.7 kcal mol<sup>-1</sup> for  $\text{R} = \text{CH}_3$ , while for  $\text{COH}^+\cdots\text{Ar}$  at MP2(full)/6-311++G(3df,3pd) the barrier is only 2.0 kcal mol<sup>-1</sup>. These findings indicate noble gas atoms may catalyze the rearrangement of cations rather than simply cool them by collisions.

### Introduction

There are several examples of the efficient conversion of high-energy ions into lower energy isomers by interaction with a neutral molecule.<sup>1</sup> For example,  $\text{HOC}^+$  reacts with  $\text{H}_2$  to give, as one channel, the lower energy isomer  $\text{HCO}^+$ .<sup>2</sup> Similarly, both CO and  $\text{CO}_2$  catalyze the interconversion of  $\text{HCN}^+$  and  $\text{CNH}^+$ ,<sup>3</sup> NO assists in the conversion of  $\text{HNNO}^+$  into  $\text{NNOH}^+$  (prior to dissociation into  $\text{N}_2$  and  $\text{OH}^+$ ),<sup>4,5</sup> and there are several examples of neutral molecules catalyzing the conversion of radical cations into isomeric distonic ions.<sup>6</sup> In each of these examples there is a substantial barrier to the proton shift and the occurrences of these reactions have been explained in terms of the “back and forth” mechanism outlined in Scheme 1.<sup>4</sup> Base M first “solvates” the higher energy isomer  $\text{XYH}^+$  and then plucks off the proton to form ion  $\text{HM}^+$ , which is “solvated” by XY through Y. Rotation of the neutral XY fragment in this complex to form  $\text{HM}^+$  “solvated” by XY through X followed by transfer of the proton to X and subsequent dissociation results in formation of the lower energy isomer  $\text{YXH}^+$ . Since there is little or no barrier to proton-transfer reactions, the requirement for the above reaction sequence to occur is that the catalyst M have a proton affinity between those of atoms X and Y in molecule XY. Similarly, interconversion of cations involving the migration of a methyl group may also be catalyzed by neutral molecules having methyl cation affinities between those of the two sites for methylation in a molecule, and recently, it was shown that Xe and  $\text{N}_2$  catalyze the rearrangement of  $\text{CH}_3\text{NO}_2^+$  into  $\text{CH}_3\text{ONO}^+$ .<sup>7</sup>

Here, we examine the effect of catalysts on the rearrangement of  $\text{COR}^+$  into  $\text{RCO}^+$  ( $\text{R} = \text{H}$  and  $\text{CH}_3$ ). Both the proton<sup>8</sup> and

### SCHEME 1



methyl cation<sup>9</sup> affinities of  $\text{N}_2$  are between those of the C and O of CO,<sup>10–13</sup> and  $\text{N}_2$  should therefore be capable of functioning as a catalyst for the interconversion of  $\text{COR}^+$  and  $\text{RCO}^+$ . A more interesting possibility is that molecules that have lower proton affinities than the oxygen atom of CO may function as catalysts by preferentially stabilizing the transition structure. Noble gas atoms are possible candidates for such a catalytic role and complexes  $\text{M}\cdots\text{HCO}^+$ , where  $\text{X} = \text{He}^{14}$  and  $\text{X} = \text{Ar}^{15}$  have recently been studied by infrared spectroscopy and both  $\text{He}\cdots\text{HCO}^+$  and  $\text{Ar}\cdots\text{HCO}^+$  have also been the subject of a recent high-level molecular orbital theoretical treatment.<sup>16</sup> Both ions were found to be linear, and  $\text{Ar}\cdots\text{HCO}^+$  was calculated to have a dissociation energy of 3.5 kcal mol<sup>-1</sup> after inclusion of a correction of 0.7 kcal mol<sup>-1</sup> for basis set superposition errors. Argon has a considerably higher proton affinity than helium and is therefore a better potential catalyst for the rearrangement of  $\text{COR}^+$ . The proton affinity of argon (calculated to be 90.6 kcal mol<sup>-1</sup><sup>17</sup>) is lower than that of the oxygen of CO (estimated to be 104.2 kcal mol<sup>-1</sup> by combining the experimental proton affinity for CO of 141.9 kcal mol<sup>-1</sup>,<sup>10</sup> where protonation occurs on carbon, and the calculated difference in proton affinities of the two atoms<sup>11</sup>), and consequently, the  $\text{COH}^+\cdots\text{Ar}$  complex is expected to have a higher binding energy than  $\text{Ar}\cdots\text{HCO}^+$ . Furthermore, the transition structure for interconversion of  $\text{COH}^+$  and  $\text{HCO}^+$  has the proton less tightly bound than those in the structures at the minima, and it is therefore probable that the transition structure has the largest solvation energy. The

<sup>⊗</sup> Abstract published in *Advance ACS Abstracts*, December 15, 1997.

**TABLE 1: Total Energies (hartrees) and Zero-Point Energies (kcal mol<sup>-1</sup>)**

molecule	B3LYP <sup>a</sup>	zero-point	QCI <sup>b</sup>	MP2 <sup>c</sup>
CO	-113.349 05	3.2	-113.192 78	-113.180 20
CH <sub>3</sub> <sup>+</sup>	-39.491 47	19.6	-39.415 75	
Ar	-527.553 87		-527.098 22	-527.110 26
N <sub>2</sub>	-109.559 69	3.5	-109.411 52	
ArH <sup>+</sup>	-527.698 01	3.8	-527.246 67	-527.261 00
N <sub>2</sub> H <sup>+</sup>	-109.753 50	10.0	-109.607 16	
ArCH <sub>3</sub> <sup>+</sup>	-567.072 33	22.7	-566.542 32	
N <sub>2</sub> CH <sub>3</sub> <sup>+</sup>	-149.124 97	28.3	-148.901 80	
HCO <sup>+</sup>	-113.581 82	10.3	-113.427 86	-113.420 00
COH <sup>+</sup>	-113.519 34	8.4	-113.362 95	-113.346 58
COH <sup>+</sup> <sup>d</sup>	-113.458 39	5.9	-113.303 14	-113.280 26
Ar <sup>+</sup> ...HCO <sup>+</sup>	-641.141 49	10.6	-640.532 57	-640.538 32
COH <sup>+</sup> ...Ar	-641.090 79	8.4	-640.479 32	-640.478 59
COH <sup>+</sup> ...Ar <sup>d</sup>	-641.056 21	7.1	-640.446 42	-640.450 20
N <sub>2</sub> <sup>+</sup> ...HCO <sup>+</sup>	-223.157 67	14.7	-222.855 01	
CO <sup>+</sup> ...HN <sub>2</sub> <sup>+</sup>	-223.125 97	13.7	-222.821 68	
COH <sup>+</sup> ...N <sub>2</sub> <sup>d</sup>	-223.105 78	13.6	-222.803 94	
CH <sub>3</sub> CO <sup>+</sup>	-152.969 68	27.9	-152.737 53	
COCH <sub>3</sub> <sup>+</sup>	-152.879 02	27.0	-152.646 68	
COCH <sub>3</sub> <sup>+</sup> <sup>d</sup>	-152.853 21	24.9	-152.619 96	
Ar <sup>+</sup> ...CH <sub>3</sub> CO <sup>+</sup>	-680.524 54	28.0		
COCH <sub>3</sub> <sup>+</sup> ...Ar	-680.434 33	27.1		
COCH <sub>3</sub> <sup>+</sup> ...Ar <sup>d</sup>	-680.422 27	26.0		
N <sub>2</sub> <sup>+</sup> ...CH <sub>3</sub> CO <sup>+</sup>	-262.534 72	32.0		
CO <sup>+</sup> ...CH <sub>3</sub> N <sub>2</sub> <sup>+</sup>	-262.477 92	31.8		
N <sub>2</sub> <sup>+</sup> ...CH <sub>3</sub> <sup>+</sup> ...CO <sup>d</sup>	-262.465 13	31.5		

<sup>a</sup> B3LYP/6-311++G(d,p). <sup>b</sup> QCISD(T)(full)/6-311++G(2df,p).  
<sup>c</sup> MP2(full)/6-311++G(3df,3pd). <sup>d</sup> ts = transition structure.

consequence of a larger stabilization for the transition structure will be a reduction in the barrier to interconversion.

In this study we report the effect of N<sub>2</sub> and Ar on the profiles to rearrangement of  $\text{COR}^+$  where R = H and CH<sub>3</sub>.

## Computational Methods

All molecular orbital calculations were performed using Gaussian 94.<sup>18</sup> Structure optimizations were carried out using the CALCALL routine along with molecular orbital calculations employing density functional theory (DFT) at the B3LYP level.<sup>19,20</sup> The 6-311++G(d,p) basis set<sup>21–25</sup> was used for all structure optimizations, and then for the  $\text{COH}^+$  and  $\text{COH}^+\cdots\text{M}$  systems these geometries were used for single-point calculations at QCISD(T)(full)/6-311++G(2df,p).<sup>26,27</sup> For each transition state, intrinsic reaction coordinate (IRC) calculations<sup>28</sup> were performed to establish that the structure was indeed for the migration of R<sup>+</sup> from one N atom to the other and not for transferring R<sup>+</sup> from N<sub>2</sub> to the catalyst. To check further the validity of the DFT calculations, the critical points on the  $\text{COH}^+$  and  $\text{COH}^+\cdots\text{Ar}$  potential energy surfaces were subjected to structure optimizations at MP2(full)/6-311++G(3df,3pd).<sup>29</sup>

The overall conclusions on the relative energies of reactants and transition states from the two different levels of theory for  $\text{COH}^+\cdots\text{M}$  were very similar, and consequently, we decided that it was unnecessary to perform QCI calculations on the larger  $\text{COCH}_3^+\cdots\text{M}$  ions. All the computed energies are given in Table 1, and the optimized structures are given in Figures 1 and 2.

## Results and Discussion

(a) **Structures.** (i)  $\text{CO}$ ,  $\text{HCO}^+$  (1),  $\text{COH}^+$  Transition Structure (2), and  $\text{COH}^+$  (3). The optimized structures for CO, HCO<sup>+</sup>, and COH<sup>+</sup> given in Figure 1 are in excellent agreement with those from previous theoretical studies<sup>11,30</sup> and also with experimental  $r_e$  values (for HCO<sup>+</sup>, C–H is 1.0972 Å and C–O is 1.1047 Å;<sup>31</sup> for COH<sup>+</sup>, O–H is 0.975 Å and C–O is 1.1570

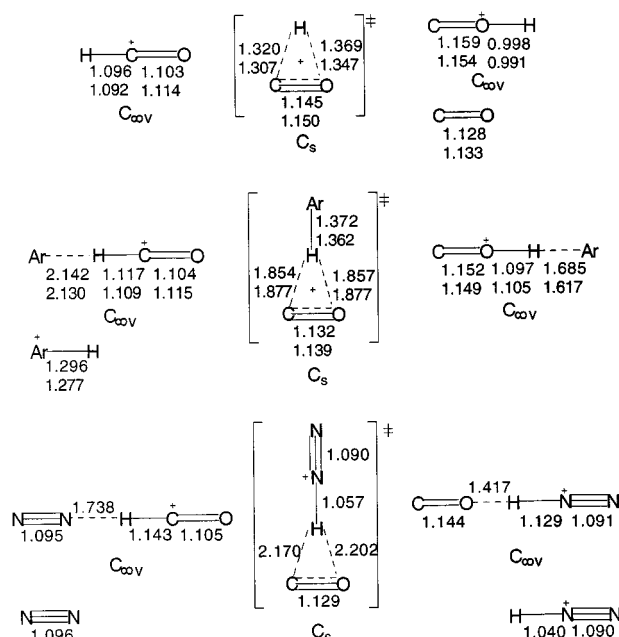


**Figure 1.** Geometric parameters for  $\text{HCO}^+\cdots\text{M}$  ions. Bond lengths are in angstroms and angles are in degrees. Higher numbers are at B3LYP/6-311++G(d,p) and lower ones at MP2(full)/6-311++G(3df,3pd).

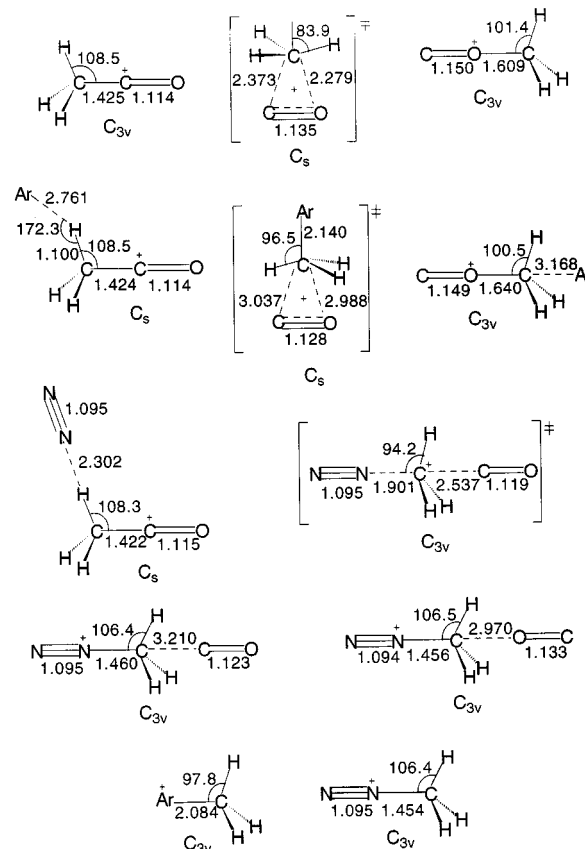
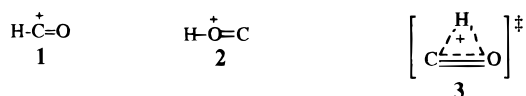


**Figure 2.** Geometric parameters for  $\text{CH}_3\text{CO}^+\cdots\text{M}$  ions. Bond lengths are in angstroms and angles are in degrees.

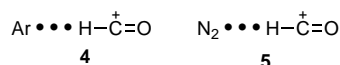
Å<sup>32</sup>). The structural changes accompanying protonation of CO, namely, shortening of the C–O distance by protonation on C and lengthening of this distance by protonation on O, have been noted previously and will not be discussed in detail here. Similarly, previous Hartree–Fock level calculations<sup>14</sup> gave COH<sup>+</sup> to be bent, but inclusion of electron correlation leads to

a linear structure for this ion. Optimization at B3LYP/6-



311++G(d,p) also gave  $\text{COH}^+$  to be linear, but bending requires little energy as shown by the low frequencies for the degenerate bending vibrations. The transition structure for interconversion between  $\text{COH}^+$  and  $\text{HCO}^+$  has a C–O distance between those in the two ions, but, consistent with Hammond's postulate,<sup>33</sup> it is closer to that in the higher energy isomer  $\text{COH}^+$ . The O–H distance, however, is larger than C–H, indicating that, on rearrangement of  $\text{COH}^+$ , H migration is well under way in the transition structure. This is consistent with the low bending frequencies calculated for  $\text{COH}^+$ .

(ii) *Ions  $M \cdots \text{HCO}^+$* . Interaction with argon and with dinitrogen results in changes to structures **1**–**3**, and the magnitude of the changes is dependent upon the proton affinity of the interacting molecule. For example, argon has a much lower proton affinity than the C of CO and interacts only very weakly with the proton, as shown by the large  $\text{Ar} \cdots \text{H}$  distance in **4** of 2.142 Å (the experimental value of 2.13 Å<sup>15</sup> is reproduced at MP2(full)/6-311++G(3df,3pd)). This interaction



results in slight elongations of the H–C and C–O distances of 0.021 and 0.001 Å, respectively. The stabilization of **4** relative to the separated species Ar and  $\text{HCO}^+$  is 3.5 kcal mol<sup>-1</sup> at B3LYP/6-311++G(d,p), 4.0 kcal mol<sup>-1</sup> at QCISD(T)(full)/6-311++G(2df,p), and 4.8 kcal mol<sup>-1</sup> at MP2(full)/6-311++G(3df,3pd). These dissociation energies do not compensate for basis set superposition errors and will therefore be slightly too high. Previous calculations on this complexed ion showed the counterpoise correction to be 0.6–0.8 kcal mol<sup>-1</sup> and the dissociation energy to be 3.2–4.2 kcal mol<sup>-1</sup>.<sup>16</sup>

Dinitrogen molecule has a higher proton affinity than argon, and solvation of  $\text{HCO}^+$  by  $\text{N}_2$  results in a stabilization of 9.5 kcal mol<sup>-1</sup> at B3LYP/6-311++G(d,p) and 9.2 kcal mol<sup>-1</sup> at QCISD(T)/6-311++G(2df,p). The C–H distance in **5** is longer than that in **4** and is 0.047 Å longer than in the isolated ion **1**. The  $\text{N} \cdots \text{H}$  distance of 1.738 Å in **5**, compared with a distance of 1.09 Å in the isolated  $\text{N}_2\text{H}^+$ , indicates a relatively weak interaction, and a Mulliken population analysis<sup>34</sup> showed there to be essentially no net transfer of positive charge onto the  $\text{N}_2$  molecule.

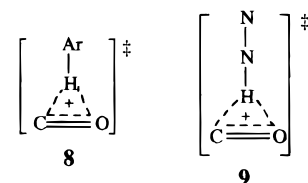
(iii) *Ions  $\text{COH}^+ \cdots M$* . The oxygen atom of CO has a proton affinity closer to that of argon, and consequently, interaction with argon is more stabilizing for  $\text{COH}^+$  than for  $\text{HCO}^+$ . The dissociation energy of **6** is calculated to be 11.8 kcal mol<sup>-1</sup> at



B3LYP/6-311++G(d,p), 12.2 kcal mol<sup>-1</sup> at QCISD(T)(full)/6-311++G(2df,p), and 14.6 kcal mol<sup>-1</sup> at MP2(full)/6-311++G(3df,3pd). At B3LYP/6-311++G(d,p), the O–H distance in **6** is 0.099 Å longer than that in the isolated ion **3** and the C–O distance is 0.007 Å shorter. Finally, the Ar–H distance (1.685 Å) in **6** is much shorter than that in **4** but is considerably longer than that in  $\text{ArH}^+$  (1.296 Å). The argon atom in **6** is calculated to have a charge of +0.26.

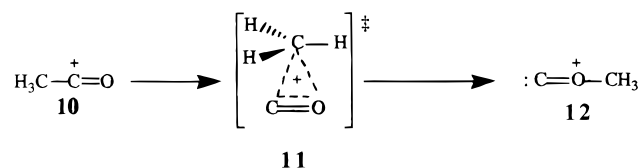
We were unable to locate a structure for ion  $\text{N}_2 \cdots \text{HOC}^+$ . All attempts at optimizing this ion resulted in migration of the proton to  $\text{N}_2$ . Ion **7**,  $\text{N}_2\text{H}^+$  “solvated” by the oxygen of CO, is at a minimum and is calculated to require 14.3 kcal mol<sup>-1</sup> at B3LYP/6-311++G(d,p) for dissociation into  $\text{N}_2\text{H}^+$  and CO. Comparison of **7** with the structure of isolated  $\text{N}_2\text{H}^+$  shows the N–H distance to be increased by 0.089 Å by interaction with OC, but the N–N distance is increased by only 0.001 Å. The C–O distance of 1.144 Å in **7** is 0.016 Å longer than that in CO, and a small amount of positive charge (+0.11) is located on the CO fragment.

(iv) *Transition Structures  $\text{COH}^+ \cdots M$* . Comparison of transition structures **8** and **9** with that for the uncatalyzed reaction



show both the C–H and O–H distances to be greatly elongated by the presence of an inert gas molecule. Structures **8** and **9** both have one imaginary frequency in which the predominant motion is displacement of the proton in a direction parallel to the C–O bond. They are best described as having the proton attached to the catalyst with this ion being solvated by the  $\pi$ -system of CO. At B3LYP/6-311++G(d,p) the dissociation energies for removal of CO from **8** and **9** are 6.8 and 2.0 kcal mol<sup>-1</sup>, respectively.

(v)  *$\text{CH}_3\text{CO}^+$  (**10**),  $\text{COCH}_3^+$  Transition Structure (**11**), and  $\text{COCH}_3^+$  (**12**)*. Addition of a methyl cation to CO results in similar but smaller changes to the C–O distance as occurs on protonation. Methylation at C then produces a decrease of 0.014 Å, while methylation at oxygen elongates the C–O distance by 0.022 Å (Figure 2). The C–C distance in **10** of 1.425 Å is



shorter than a normal C–C bond by about 0.1 Å, while the O–C distance in **12** of 1.609 Å is almost 0.2 Å longer than a characteristic C–O single bond. Transition structure **11** has large OC and CC distances, and the  $\text{CH}_3$  fragment is almost planar. These structural parameters indicate that  $\text{CH}_3^+$  is largely detached from the CO, and at B3LYP/6-311++G(d,p) the transition structure is only 6.8 kcal mol<sup>-1</sup> lower in energy than the dissociation products,  $\text{CH}_3^+$  plus CO. A Mulliken population analysis<sup>33</sup> gave a charge of +0.72 on the  $\text{CH}_3$  group in **11**.

(vi) *Ions  $M \cdots \text{CH}_3\text{CO}^+$* . Argon and dinitrogen both interact very weakly with  $\text{CH}_3\text{CO}^+$  (Ar by 0.4 kcal mol<sup>-1</sup> and  $\text{N}_2$  by 2.3 kcal mol<sup>-1</sup>). In both instances the preferred position for the “solvating” molecule is adjacent to one of the H atoms of the methyl group and not along the  $\text{C}_3$  axis of  $\text{CH}_3\text{CO}^+$ , and in both ion–molecule complexes the structure of the  $\text{CH}_3\text{CO}^+$  portion is almost identical with that of the isolated  $\text{CH}_3\text{CO}^+$  ion.

(vii) *Ions  $\text{COCH}_3^+ \cdots M$* . Ion  $\text{COCH}_3^+ \cdots \text{Ar}$  has  $\text{C}_{3v}$  symmetry. The argon is weakly attached to the methyl group as shown by the long Ar–C distance (3.168 Å) and small dissociation energy (0.6 kcal mol<sup>-1</sup>). We were unable to locate a minimum for  $\text{COCH}_3^+ \cdots \text{N}_2$  and found that  $\text{N}_2$  plucks off

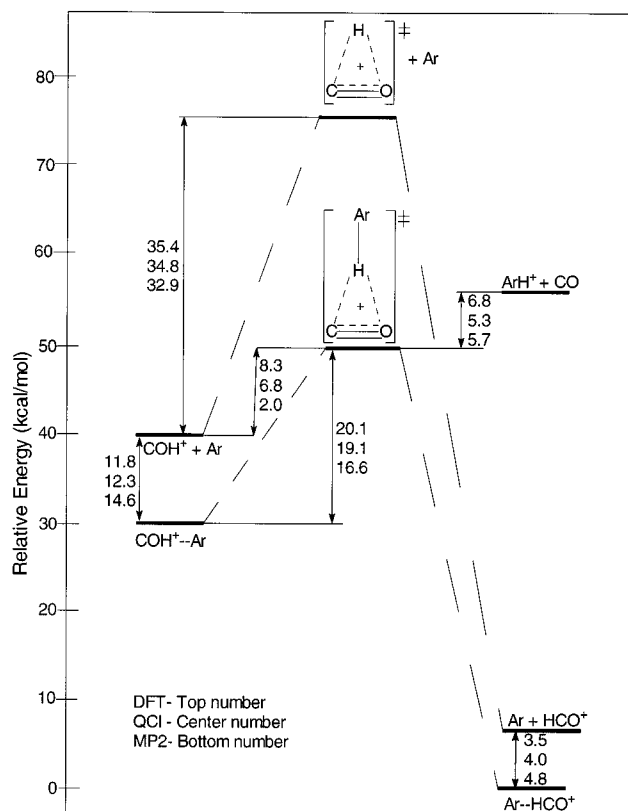


Figure 3. Reaction profile for  $\text{Ar} + \text{COH}^+$  at 298 K.

$\text{CH}_3^+$  to give  $\text{N}_2\text{CH}_3^+\cdots\text{OC}$ , a combination that is 1.6 kcal  $\text{mol}^{-1}$  lower in energy than  $\text{N}_2\text{CH}_3^+$  plus  $\text{OC}$ .

(viii) *Transition Structures  $\text{COCH}_3^+\cdots\text{M}$ .* Attachment of an argon to the methyl group of transition structure **11** resulted in increases of  $\sim 0.7$  Å in the already large C–C and C–O distances, and the complexed transition structure is only 0.5 kcal  $\text{mol}^{-1}$  lower in energy than separated  $\text{ArCH}_3^+$  plus  $\text{CO}$ . In the argon-complexed transition structure the methyl group is essentially attached to the argon, although interaction with the  $\pi$ -bond of  $\text{CO}$  results in the Ar–C distance being 0.056 Å longer than in isolated  $\text{ArCH}_3^+$  and the methyl group is slightly flattened (angle Ar–C–H is  $96.5^\circ$  compared with  $97.8^\circ$  in the isolated ion).

On the  $\text{C}_2\text{H}_3\text{ON}_2^+$  surface we were unable to locate a minimum for  $\text{N}_2\cdots\text{H}_3\text{COC}^+$ , and since interconversion between  $\text{N}_2\text{CH}_3^+\cdots\text{OC}$  and  $\text{N}_2\text{CH}_3^+\cdots\text{CO}$  proceeds through dissociation/recombination, then the only transition structure on the reaction profile is for transfer of the methyl group on  $\text{N}_2$  in  $\text{N}_2\text{CH}_3^+\cdots\text{CO}$  to the carbon atom, i.e., to form the structure at the global minimum  $\text{N}_2\cdots\text{CH}_3\text{CO}^+$ . This transition structure has long N–C (1.901 Å) and C–C (2.537 Å) distances, and the NCH angle of  $94.2^\circ$  indicates that the methyl group is closer to being planar but is still angled toward  $\text{N}_2$  rather than toward  $\text{CO}$ ; i.e., the transition structure is closer to the higher energy structure  $\text{N}_2\text{CH}_3^+\cdots\text{CO}$ .

(b) *Energetics and Profiles to Rearrangement.* The profiles for rearrangement of  $\text{COR}^+$  to  $\text{RCO}^+$  in the presence of catalysts  $\text{Ar}$  and  $\text{N}_2$ , constructed from enthalpies corrected to 298 K, are given in Figures 3–6. Each profile has different features and will therefore be discussed separately.

(i)  *$\text{COH}^+\cdots\text{Ar}$ .* For the rearrangement of  $\text{COH}^+$  to  $\text{HCO}^+$  in the absence of any catalyst, the profile is given by the upper set of energy levels in Figure 3. The barrier for the uncatalyzed reaction is 35.4 kcal  $\text{mol}^{-1}$  at B3LYP/6-311++G(d,p) and 34.8 kcal  $\text{mol}^{-1}$  at QCISD(T)(full)/6-311++G(2df,p). Addition of

an argon atom stabilizes each of the structures, with the largest effect being on the structure in which the proton is least firmly attached, the transition structure, and the smallest on the product ion  $\text{HCO}^+$ , where the proton is most strongly bound. The net effect of attaching one argon atom is to produce the profile involving only the lowest energy levels. Here, the calculated barriers are 20.1 kcal  $\text{mol}^{-1}$  (at B3LYP/6-311++G(d,p)) and 19.1 kcal  $\text{mol}^{-1}$  (at QCISD(T)(full)/6-311++G(2df,p)); i.e., the calculated barriers are reduced by about  $\sim 15$  kcal  $\text{mol}^{-1}$  from those in the uncatalyzed reaction. In solution, a large number of solvent molecules are involved in solvating an ion, and modeling such a process by only one interacting molecule is clearly insufficient to give an accurate solvation energy. However, the first solvent molecule added generally has the largest effect, and the numbers given here then provide a crude estimate of the effect of solvation by argon on this 1,2-proton migration.

The most interesting aspect of Figure 3 is for the rearrangement of  $\text{COH}^+$  in the gas phase. When  $\text{COH}^+$  and argon collide, the sum of the energies of these molecules is lower than that of the solvated transition structure by only 8.3 kcal  $\text{mol}^{-1}$  at B3LYP/6-311++G(d,p) and by 6.8 kcal  $\text{mol}^{-1}$  at QCISD(T)(full)/6-311++G(2df,p); i.e., the effective barrier to rearrangement of  $\text{COH}^+$  is drastically reduced by using argon as a catalyst in the gas phase. Furthermore, if the colliding atom and ion are hot, then a significant fraction of  $\text{COH}^+$  may be induced to rearrange to  $\text{HCO}^+$  during the course of the collision. Such a rearrangement has important implications for gas-phase ion–molecule chemistry where collisions with noble gas atoms are frequently used to thermally stabilize ions. Our findings now suggest that, depending upon the proximity of  $\text{R}^+$  affinities, noble gas atoms may in fact catalyze the rearrangement of an ion rather than simply cool it by collisions.

(ii)  *$\text{CO}\cdots\text{HN}_2^+$ .*  $\text{N}_2$  has a higher proton affinity than the oxygen atom of  $\text{CO}$ , and we found that there is no barrier to proton transfer from  $\text{COH}^+$  to  $\text{N}_2$ . Ion–molecule complex  $\text{COH}^+\cdots\text{N}_2$  therefore does not exist, and in this system the lowest energy levels on the profile in Figure 4 are for  $\text{CO}\cdots\text{HN}_2^+$  rearranging, through a transition structure that resembles  $\text{N}_2\text{H}^+$  interacting with the  $\pi$ -system of  $\text{CO}$ , to the structure at the global minimum,  $\text{N}_2\cdots\text{HCO}^+$ . The barrier to this process is 12.3 kcal  $\text{mol}^{-1}$  at B3LYP/6-311++G(d,p) and 10.7 kcal  $\text{mol}^{-1}$  at QCISD(T)(full)/6-311++G(2df,p).

In the gas phase a collision between  $\text{COH}^+$  and  $\text{N}_2$  will simply result in transfer of the proton to  $\text{N}_2$ , and this will be followed by a transfer back to the carbon of  $\text{CO}$ . Both these transfers are exothermic, and conversion of  $\text{COH}^+$  to  $\text{HCO}^+$  then should be efficiently catalyzed by  $\text{N}_2$ .

(iii)  *$\text{COCH}_3^+\cdots\text{Ar}$ .* For the uncatalyzed reaction, the barrier to 1,2-methyl migration in  $\text{COCH}_3^+$  is 14.2 kcal  $\text{mol}^{-1}$  at B3LYP/6-311++G(d,p) (upper profile in Figure 5). This is compared with a value of 35.4 kcal  $\text{mol}^{-1}$  for the 1,2-proton shift, and the much smaller barrier is attributed to the greater ability of  $\text{CH}_3$  (relative to H) to carry the positive charge in the transition structure.

The methyl cation affinities of both atoms in  $\text{CO}$  are higher than that of argon, and interaction with an argon atom has little stabilizing effect on both  $\text{CH}_3\text{CO}^+$  and  $\text{COCH}_3^+$  (both are less than 1 kcal  $\text{mol}^{-1}$ ). However, argon interacts more strongly with the methyl group in the transition structure and the overall effect is to reduce the barrier for the gas-phase reaction to 5.7 from 14.2 kcal  $\text{mol}^{-1}$ .

(iv)  *$\text{CO}\cdots\text{CH}_3\text{N}_2^+$ .* The methyl cation affinity of  $\text{N}_2$  is between those of O and C in  $\text{CO}$ , and consequently, as in the

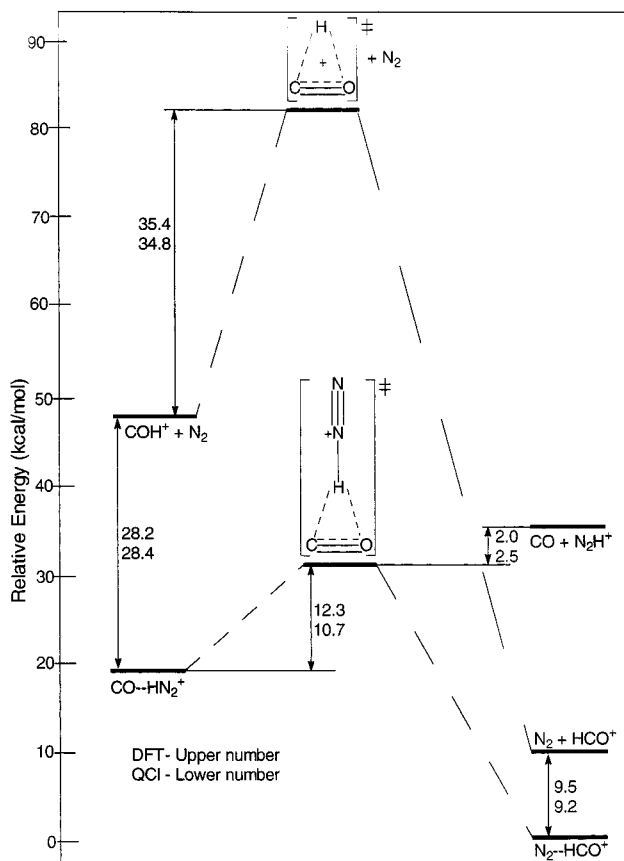


**Figure 4.** Reaction profile for  $N_2 + COH^+$  at 298 K.

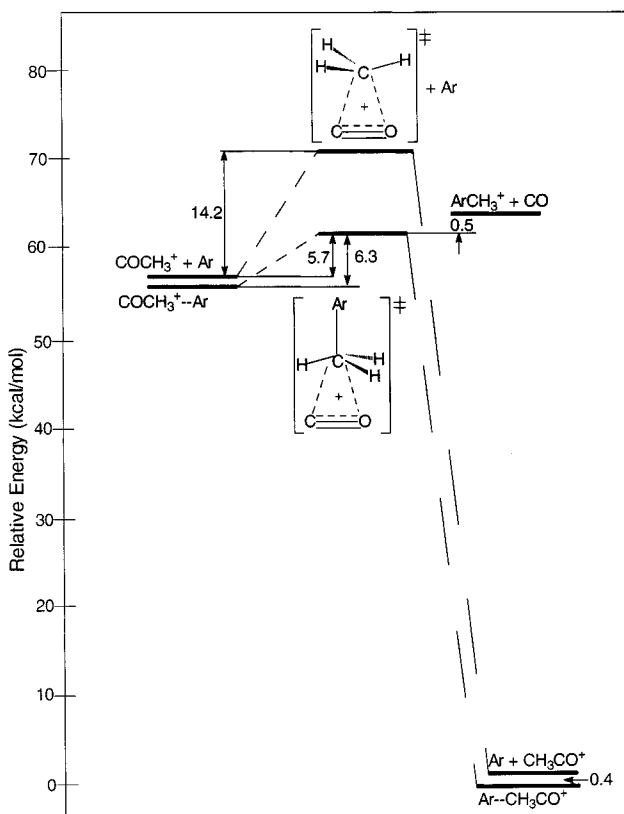


**Figure 5.** Reaction profile for  $Ar + COCH_3^+$  at 298 K.

case of rearrangement in  $COH^+$  catalyzed by  $N_2$ , the 1,2-migration of  $CH_3^+$  can occur simply by transfer of  $CH_3^+$  from  $COCH_3^+$  to  $N_2$  and then switching the  $CH_3^+$  back to the C of

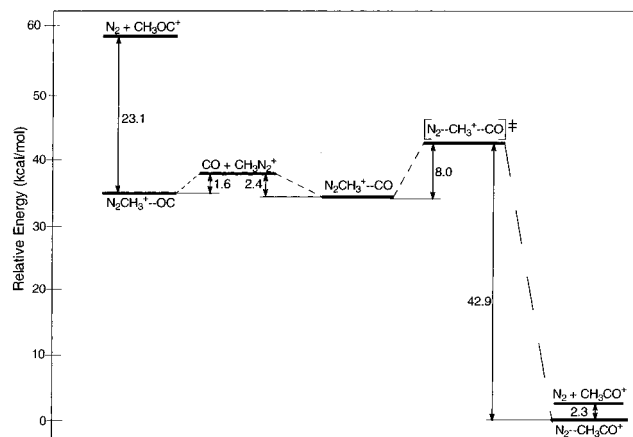


**Figure 6.** Reaction profile for  $N_2 + COCH_3^+$  at 298 K.

**TABLE 2: Barriers<sup>a</sup> to the 1,2-Migration of  $R^+$  in  $COR^+$**

molecular combination	B3LYP <sup>b</sup>	QCISD <sup>c</sup>	MP2 <sup>d</sup>
(a) Proton ( $R = H^+$ )			
(i) from $COH^+ + M$			
no catalyst	35.4	34.8	32.9
$COH^+ + Ar$	8.3	6.8	2.0
$COH^+ + N_2$	-15.9	-17.7	
(ii) from $COH^+ \cdots M$			
$COH^+ \cdots Ar$	20.1	19.1	16.6
$COH^+ \cdots N_2$	12.3	10.7	
(b) Methyl Cation ( $R = CH_3^+$ )			
(i) from $COCH_3^+ + M$			
no catalyst	14.2	14.8	
$COCH_3^+ + Ar$	5.7		
$COCH_3^+ + N_2$	-16.0		
(ii) from $COCH_3^+ \cdots M$			
$COCH_3^+ \cdots Ar$	6.3		
$CO \cdots CH_3N_2^+$	7.2		

<sup>a</sup> In kcal mol<sup>-1</sup>. <sup>b</sup> B3LYP/6-311++G(d,p). <sup>c</sup> QCISD(T)(full)/6-311++G(2df,p). <sup>d</sup> MP2(full)/6-311++G(3df,3pd).

CO. In the latter step there is a barrier of 5.6 kcal mol<sup>-1</sup>, but the transition structure to this process is much lower in energy than the initial reactants  $N_2$  and  $CH_3OC^+$ .

$N_2CH_3^+$  forms weakly bound complexes with CO, with a slight preference for binding to carbon. Rearrangement of  $N_2-CH_3^+ \cdots CO$  to  $N_2$  plus  $CH_3CO^+$  involves a transition structure in which  $CH_3^+$  is loosely bound to both  $N_2$  and CO and lies 8 kcal mol<sup>-1</sup> above  $N_2CH_3^+ \cdots CO$ .

## Conclusions

The proton and methyl cation affinities of  $N_2$  are higher than those of the oxygen of CO but lower than those of the carbon.  $N_2$  then plucks off R from  $COR^+$  ( $R = H, CH_3$ ) and returns it to the carbon atom, thereby converting  $COR^+$  into  $RCO^+$ . Assuming that the intermediate ion-molecule complexes are not stabilized by collisions, then these  $N_2$ -assisted processes both occur without barriers. These reactions are examples of the "back and forth" mechanism proposed by Ferguson.

Argon has lower proton and methyl cation affinities than both oxygen and carbon of CO and therefore cannot fully remove  $R^+$  from the oxygen atom. However, argon forms ion-atom complexes with  $COR^+$  and  $RCO^+$  ( $R = H, CH_3$ ) and also with the transition structures for their interconversion, and the stabilizations arising from these interactions are largest in the transition structures. The net effect on the reaction profile of including one argon atom attached to each structure is to reduce the barriers to rearrangement from around 35 to about 20 kcal mol<sup>-1</sup> when  $R = H$  and from 14.2 to 6.3 kcal mol<sup>-1</sup> when  $R =$

$\text{CH}_3$ . Furthermore, gas-phase reactants  $\text{COR}^+$  and argon are only slightly lower in energy than the solvated transition structure  $\text{COR}^+\cdots\text{Ar}$ , and this raises the possibility that in some collisions between Ar and  $\text{COR}^+$  rearrangement to  $\text{RCO}^+$  will occur. Argon is frequently used in gas-phase ion–molecule chemistry to thermally stabilize ions by collisions. The results of our theoretical studies indicate that experimentalists should be aware that argon can in some systems function as a catalyst to convert ions into lower energy isomers.

**Acknowledgment.** We thank Steve Quan for much technical assistance in our computational work. Continued financial support from the Natural Science and Engineering Council of Canada is much appreciated.

## References and Notes

- (1) Bohme, D. K. *Int. J. Mass Spectrom. Ion Processes* **1992**, *115*, 95.
- (2) Freeman, C. G.; Knight, J. S.; Love, J. G.; McEwan, M. J. *Int. J. Mass Spectrom. Ion Processes* **1987**, *80*, 255.
- (3) Petrie, S.; Freeman, C. G.; Maut-Ner, G.; Ferguson, E. E. *J. Am. Chem. Soc.* **1990**, *112*, 7121.
- (4) Ferguson, E. E. *Chem. Phys. Lett.* **1989**, *156*, 319.
- (5) Jones, T. T. C.; Raouf, A. S. M.; Birkinshaw, K.; Twiddy, N. D. *J. Phys. B* **1981**, *14*, 2713.
- (6) Audier, H. E.; Leblanc, D.; Mougues, P.; McMahon, T. B.; Hammerum, S. J. *Chem. Soc., Chem. Commun.* **1994**, 2329.
- (7) Baranov, V.; Petrie, S.; Bohme, D. K. *J. Am. Chem. Soc.* **1996**, *118*, 4500.
- (8) Szulejko, J. E.; McMahon, T. B. *J. Am. Chem. Soc.* **1993**, *115*, 7839.
- (9) Glukhovtsev, M. N.; Szulejko, J. E.; McMahon, T. B.; Gauld, J. W.; Scott, A. P.; Smith, B. J.; Pross, A.; Radom, L. *J. Phys. Chem.* **1994**, *98*, 13099.
- (10) Lias, S. G.; Bartmess, J. E.; Liebman, J. F.; Holmes, J. L.; Levin, R. D.; Mallard, W. G. *J. Phys. Chem. Ref. Data, Suppl. 1* **1988**, *17*.
- (11) Yamaguchi, Y.; Richards, C. A., Jr.; Schaefer, H. F., III. *J. Chem. Phys.* **1994**, *101*, 8945.
- (12) Nobes, R. H.; Bouma, W. J.; Radom, L. *J. Am. Chem. Soc.* **1983**, *105*, 309.
- (13) Nobes, R. H.; Radom, L. *Org. Mass Spectrom.* **1986**, *21*, 407.
- (14) Nikorodov, S. A.; Maier, J. P.; Bieske, E. J. *J. Chem. Phys.* **1995**, *103*, 1297.
- (15) Nikorodov, S. A.; Dopfer, O.; Ruchti, T.; Meuwly, M.; Maier, J. P.; Bieske, E. J. *J. Phys. Chem.* **1995**, *99*, 17188.
- (16) Nowek, A.; Leszczynski, J. *J. Chem. Phys.* **1996**, *105*, 6388.
- (17) Rosmus, P. *Theor. Chim. Acta* **1979**, *51*, 359.
- (18) Frisch, M. J.; Trucks, G. W.; Schlegel, H. B.; Gill, P. M. W.; Johnson, B. G.; Robb, M. A.; Cheeseman, J. R.; Keith, T.; Petersson, G. A.; Montgomery, J. A.; Raghavachari, K.; Al-Laham, M. A.; Zakrzewski, V. G.; Ortiz, J. V.; Foresman, J. B.; Cioslowski, J.; Stevanov, B. B.; Nanayakkara, A.; Challacombe, M.; Peng, C. Y.; Ayala, P. Y.; Chen, W.; Wong, M. W.; Andres, J. L.; Repogle, E. S.; Gomperts, R.; Martin, R. L.; Fox, D. J.; Binkley, J. S.; Defrees, D. J.; Baker, J.; Stewart, J. P.; Head-Gordon, M.; Gonzalez, C.; Pople, J. A. *Gaussian 94*; Gaussian Inc.: Pittsburgh, PA, 1995.
- (19) Becke, A. D. *J. Chem. Phys.* **1993**, *93*, 5648.
- (20) Lee, C.; Yang, W.; Parr, R. G. *Phys. Rev. B* **1988**, *37*, 785. (b) Miehlich, B.; Savin, A.; Stoll, H.; Preuss, H. *Chem. Phys. Lett.* **1989**, *157*, 200.
- (21) Krishnan, R.; Binkley, J. S.; Seeger, R.; Pople, J. A. *J. Chem. Phys.* **1980**, *72*, 650.
- (22) McLean, A. D.; Chandler, G. S. *J. Chem. Phys.* **1980**, *72*, 5639.
- (23) Chandrasekhar, J.; Andrade, J. G.; Schleyer, P. v. R. *J. Am. Chem. Soc.* **1981**, *103*, 5609.
- (24) Chandrasekhar, J.; Spitznagel, G. W.; Schleyer, P. v. R. *J. Comput. Chem.* **1983**, *4*, 294.
- (25) Curtiss, L. A.; McGrath, M. P.; Blaudeau, J. P.; Davis, N. E.; Binning, R. C., Jr.; Radom, L. *J. Chem. Phys.* **1995**, *103*, 6104.
- (26) (a) Pople, J. A.; Head-Gordon, M.; Raghavachari, K. *J. Chem. Phys.* **1987**, *87*, 5968. (b) Pople, J. A.; Head-Gordon, M.; Raghavachari, K. *J. Chem. Phys.* **1989**, *90*, 4635. (c) Raghavachari, K.; Head-Gordon, M.; Pople, J. A. *J. Chem. Phys.* **1990**, *93*, 1486.
- (27) Frisch, M. J.; Pople, J. A.; Binkley, J. S. *J. Chem. Phys.* **1984**, *80*, 3265.
- (28) Gonzalez, C.; Schlegel, H. B. *J. Chem. Phys.* **1989**, *90*, 2154.
- (29) (a) Moller, C.; Plesset, M. S. *Phys. Rev.* **1934**, *46*, 618. (b) Pople, J. A.; Binkley, J. S.; Seeger, R. *Int. J. Quantum Chem. Symp.* **1976**, *10*, 1.
- (30) Ma, N. L.; Smith, B. J.; Radom, L. *Chem. Phys. Lett.* **1992**, *197*, 581.
- (31) Woods, R. C. *Philos. Trans. R. Soc. London. Ser. A* **1988**, *342*, 141.
- (32) Berry, R. J.; Harmony, M. D. *J. Mol. Spectrosc.* **1988**, *128*, 176.
- (33) Hammond, G. S. *J. Am. Chem. Soc.* **1955**, *77*, 334.
- (34) Mulliken, R. S. *J. Chem. Phys.* **1955**, *23*, 1833, 1841, 2338, 2343.